

Minimal Path on the Hierarchical Diamond Lattice

Stéphane Roux,^{1,5} Alex Hansen,² Luciano R. da Silva,³ Liacir S. Lucena,³ and Ras B. Pandey⁴

Received March 5, 1991; final April 30, 1991

We consider the minimal paths on a hierarchical diamond lattice, where bonds are assigned a random weight. Depending on the initial distribution of weights, we find all possible asymptotic scaling properties. The different cases found are the small-disorder case, the analog of Lévy's distributions with a power-law decay at $-\infty$, and finally a limit of large disorder which can be identified as a percolation problem. The asymptotic shape of the stable distributions of weights of the minimal path are obtained, as well as their scaling properties. As a side result, we obtain the asymptotic form of the distribution of effective percolation thresholds for finite-size hierarchical lattices.

KEY WORDS: Minimal path; directed polymer; hierarchical lattice; percolation.

1. INTRODUCTION

The minimal path problem in a random geometry is a very general problem encountered in many different fields of physics. Some recently studied problems single out this concept: namely, the structure of random fronts arising in ballistic deposition models or in the frontier of Eden

¹ Centre d'Enseignement et de Recherche en Analyse des Matériaux, École Nationale des Ponts et Chaussées, F-93167 Noisy-le-Grand Cédex, France.

² Fysisk Institutt, Universitetet i Oslo, N-0316 Oslo 3, Norway.

³ Departamento de Física, Universidade Federal do Rio Grande do Norte, Natal, RN, 59072 Brazil.

⁴ Department of Physics and Astronomy, University of Southern Mississippi, Hattiesburg, Mississippi 39406-5046.

⁵ Also at Laboratoire de Physique et Mécanique des Milieux Hétérogènes, URA CNRS 847, École Supérieure de Physique et Chimie Industrielles, Paris Cédex 05, France.

cluster,⁽¹⁾ the conformation of directed polymers at zero temperature,⁽²⁾ the transport properties of nonlinear systems,⁽³⁾ etc. The scaling properties of this problem have been solved exactly in two dimensions, for the case of a small disorder.⁽⁴⁾ Various conjectures have been suggested for higher dimensions^(2,5-7); however, the problem is still open in these dimensions.

Even in the simple case of the two-dimensional Euclidian lattice, all studies have dealt with a “small” disorder, assuming that the asymptotic properties of the system would not depend on the distribution one starts with. We address in this paper the question of the unicity of the “fixed point” toward which the system converges in the thermodynamic limit (i.e., when the lattice size goes to infinity).

We carried out our study in a very simple geometry: a hierarchical diamond lattice. This type of geometry has already been considered by Derrida and Griffiths⁽⁸⁾ and Halpin-Healy.⁽⁹⁾ This structure allows a very simple and elegant formulation of the problem. In addition, it shares a lot of common features with Euclidian lattices. Although the numerical values of the exponents obtained cannot in principle be directly compared, it appears that the values of the exponents obtained in this simple geometry are extremely close to the values obtained for a Euclidian lattice, as demonstrated in ref. 9, and discussed in the present article.

The paper is organized as follows: A brief presentation of the problem is given in Section 2, in terms of the scaling transformation of a distribution of local weights, similar to the way the problem is presented by Derrida and Griffiths⁽⁸⁾ and Halpin-Healy.⁽⁹⁾ In Section 3, we recall briefly some basic results relative to the stability of the sum of random variables, which corresponds to the simple one-dimensional case (and also the limit of infinite dimension). Section 4 gives the stable laws, in a number of steps. Section 4.1 contains the definition of our notation of the scaling indices; Section 4.2 gives the recursion transformation of the distribution when the size is scaled by a factor of two. The stability of the power-law decay of the distribution close to plus or minus infinity is discussed respectively in Sections 4.3 and 4.4; and finally Section 4.5 gives the asymptotic shape of the distribution for small and large arguments in the generic case (termed “small-disorder” case). In Section 5, we discuss more specifically the scaling properties of the small-disorder case, and propose a relation which relies on the validity of a simplification. An unstable fixed point which can be identified with a percolation problem is analyzed in Section 6, and some numerical simulations are presented in Section 7. Section 8 makes the link with related works published recently on the breakdown of universality for directed polymers. Section 9 summarizes the main results obtained or conjectured in this paper.

2. PRESENTATION OF THE PROBLEM

The geometry of the hierarchical diamond lattice is shown in Fig. 1. The starting structure, say the zeroth generation, is a simple bond. To go from one generation to the next, one substitutes each bond by four bonds assembled in a diamond shape. The number of bonds in the structure at the n th generation is simply 4^n , and its length is 2^n . The “dimensionality” of the lattice is thus 2.

In a given lattice, we assign to each bond i a random number x_i picked according to a distribution $f_0(x)$. All paths \mathcal{P} which cross the system are given a weight $\|\mathcal{P}\|_1$ which is the sum of all numbers x along the path:

$$\|\mathcal{P}\|_1 = \sum_{i \in \mathcal{P}} x_i \tag{1}$$

We now consider the path $\tilde{\mathcal{P}}$ which minimizes the above norm over the set of all paths. We call $\alpha_1(L)$ the minimal weight per unit length

$$\alpha_1(L) = \frac{\|\tilde{\mathcal{P}}\|_1}{L} = \frac{\min_{\mathcal{P}} \|\mathcal{P}\|_1}{L} \tag{2}$$

where L is the length of the lattice. We are interested in the statistical distribution of α_1 in the limit $L \rightarrow \infty$.

Before studying this problem, we would like to make clear its connec-

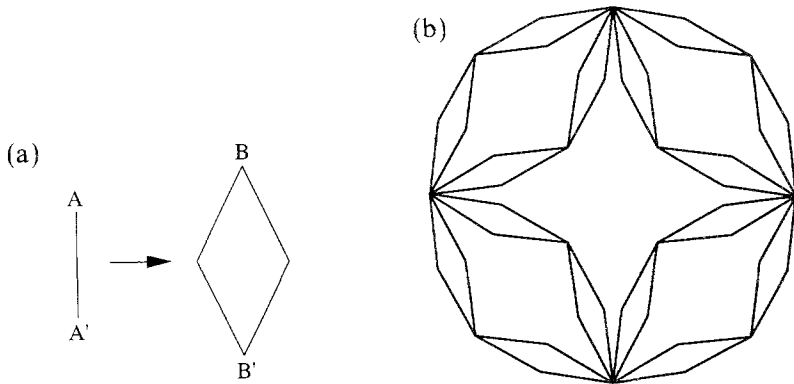


Fig. 1. Geometry of the hierarchical diamond lattice. (a) To go from one generation to the following, one replaces all bonds by a diamond of four bonds. (b) The lattice at the third generation.

tion with percolation. In order to establish it, we propose to generalize the initial formulation. Let us consider the following norm over paths:

$$\|\mathcal{P}\|_a = \left(\sum_{i \in \mathcal{P}} x_i^a \right)^{1/a} \quad (3)$$

We introduce $\alpha_a(L)$ as previously:

$$\alpha_a(L) = \frac{\min_{\mathcal{P}} \|\mathcal{P}\|_a}{L^{1/a}} \quad (4)$$

where the $L^{-1/a}$ factor is included to have α_a independent of L for a Dirac distribution of x 's.

In the limit case where a tends to infinity, the norm $\|\mathcal{P}\|_a$ has a simple expression: it tends toward the maximum of the weight of the bonds in the path:

$$\|\mathcal{P}\|_{\infty} = \max_{i \in \mathcal{P}} (x_i) \quad (5)$$

and thus $\alpha_{\infty}(L)$ is

$$\alpha_{\infty}(L) = \min_{\mathcal{P}} (\max_{i \in \mathcal{P}} (x_i)) \quad (6)$$

It is easy to relate this last expression to the effective percolation threshold of the lattice.⁽¹⁰⁾ If one thinks of the random numbers x_i as heights of barriers, then $\alpha_{\infty}(L)$ can be interpreted as the smallest height which is necessary to overpass in order to get from one end of the lattice to the other. If the x 's were picked from a uniform distribution between 0 and 1, it is thus possible to interpret $\alpha_{\infty}(L)$ as an effective percolation threshold. If the distribution of x is f_0 , we may relate $\alpha_{\infty}(L)$ to the effective percolation threshold $p_c(L)$ in the following way: Let F_0 be the cumulative distribution of x 's, $dF_0/dx = f_0$. Then we have

$$F_0(\alpha_{\infty}(L)) = p_c(L) \quad (7)$$

and thus

$$\alpha_{\infty}(L) = F_0^{-1}(p_c(L)) \quad (8)$$

In this simple percolation limit, we can easily obtain the asymptotic shape of the distribution of effective threshold for finite-size lattices and we will show that percolation is a limit fixed point of the minimal path problem even for $a = 1$.

The structure of the hierarchical lattice allows us to obtain the expression of the distribution $f_{(n+1)}(x)$ of weights of minimal path knowing the distribution of the previous generation $f_n(x)$. It can be obtained from the simple steps that are needed to construct a lattice at the $(n + 1)$ th generation from lattices at the n th generation: the combination of lattices in *series* and then in *parallel*.

Series. The weight y of the minimal path spanning two lattices connected in series is simply the sum of the two weights x_1 and x_2 of the minimal path in each lattice,

$$y = x_1 + x_2 \tag{9}$$

If $f_n(x)$ is the distribution of the weights x_i , the distribution of y , $\phi(y)$, is given by the convolution of f_n with itself:

$$\begin{aligned} \phi &= f_n * f_n = \mathcal{L}(f_n) \\ \phi(y) &= \int_{-\infty}^{\infty} f_n(y-x) f_n(x) dx \end{aligned} \tag{10}$$

Parallel. For two lattices connected in parallel, the weight z of the minimal path is simply the minimum of the two weights y_1 and y_2 of the minimal path in each lattice,

$$z = \min(y_1, y_2) \tag{11}$$

The distribution of z , $\psi(z)$, is given by

$$\psi(z) = 2\phi(z) \int_z^{\infty} \phi(y) dy = \mathcal{P}(\phi)(z) \tag{12}$$

Rescaling. Finally, we want to divide the minimal weight by the lattice size; thus we introduce a last transformation:

$$\zeta(z) = 2\psi(2z) = \mathcal{L}(\psi)(z) \tag{13}$$

We thus obtain the following transformation at each generation:

$$f_{n+1} = \mathcal{L}(\mathcal{P}(\mathcal{L}(f_n))) \tag{14}$$

In the following, we will investigate the fixed points of this transformation and the asymptotic shape of the distribution for large n . However, before proceeding, we want to recall some well-known results relative to the one-dimensional case.

3. ONE-DIMENSIONAL CASE

In this case, only the $\mathcal{L}\mathcal{S}$ transformations [Eqs. (10) and (13)] relate two consecutive distributions. The “lattice” is simply a straight line of length $L = 2^n$. The path is unique and its weight is the sum of 2^n random numbers distributed according to a distribution f_0 . The question we address becomes for this simple case, what is the evolution of the mean of this sum, of its deviations, and finally of the entire distribution when the length of the path goes to infinity? The fixed points of this transformation are given by the Gaussian and Lévy distributions (e.g., ref. 11). The fixed point which has the “largest” basin of attraction is the Gaussian distribution. It corresponds to the case where the second moment of the distribution f_0 is finite. In this case, the limit value of $\langle \alpha(L) \rangle = m(L)$ [Eq. (2)] is simply the mean value of f_0 :

$$m(L) = \langle \alpha(L) \rangle = \int_{-\infty}^{\infty} x f_0(x) dx \quad (15)$$

and the mean deviation of the distribution, $\sigma(L) = (\langle \alpha^2 \rangle - \langle \alpha \rangle^2)^{1/2}$, varies with L as

$$\sigma(L) \sim \sigma_0 L^{-1/2} \quad (16)$$

The asymptotic form of the distribution of α is a Gaussian.

However, when the second moment is infinite and the first is finite, then Eq. (15) holds, but Eq. (16) is replaced by

$$\sigma(L) \sim \sigma_0 L^{1/\mu-1} \quad (17)$$

This behavior is observed for instance when the initial distribution $f_0(x) \sim x^{-\mu-1}$ at infinity, for $1 < \mu < 2$.

Finally, when neither the first nor the second moment exists, then Eq. (15) is replaced by

$$m(L) \sim \alpha_0 L^{1/\mu-1} \quad (18)$$

and Eq. (17) holds for the mean deviation. This case is naturally encountered for a distribution which is equivalent to $f_0(x) \sim x^{-\mu-1}$ at infinity, for $0 < \mu < 1$. In the last two cases, the asymptotic form of the distribution is a Lévy distribution. The above picture of the one-dimensional case is a crude description that captures the most important points. We refer the reader to ref. 11 and references therein for a more rigorous treatment and explicit statements of convergence theorems.

4. FIXED POINTS

4.1. Notations

In the case of a small disorder (we will come to a more precise definition of this concept in the following), the distribution of the minimal weights f_n on a hierarchical lattice tends to a Dirac distribution when the lattice size tends to infinity. The way f_n approaches this limit is interesting. More precisely, if we translate the distribution and rescale it, we find that for large n , f_n approaches a well-defined distribution $\varphi(x)$ which satisfies:

$$\mathcal{LPS}\varphi(x) = a\varphi(ax + b) \tag{19}$$

where α and b are two scalars which are characteristic of the problem. a can be understood as an eigenvalue, whereas φ is an eigenfunction. This form has been introduced by Derrida and Griffiths.⁽⁸⁾ In simple words, asymptotically, the transformation, \mathcal{LPS} is the combination of a dilation of ratio a and of a translation by b .

From Eq. (19), it is easy to verify that the integral of φ is constant (it remains equal to one). Computing the first moment m' and the mean deviation σ' of the transformed distribution as a function of the initial one, m and σ , we obtain the following relations:

$$m' = \frac{m - b}{a} \tag{20}$$

$$\sigma' = \frac{\sigma}{a}$$

The transformation changes the size of the lattice by a factor of two. However, the distribution f_n changes its width by a factor of a . This defines⁶ a correlation length exponent $1/\nu = \log(a)/\log(2)$. Thus we may write

$$\sigma \propto L^{-1/\nu} \tag{21}$$

We also obtain the scaling of the difference between the first moment and its asymptotic value m_∞ :

$$m - m_\infty \propto L^{-1/\nu} \tag{22}$$

where the same exponent ν applies.

⁶ In a Euclidian lattice, it can be shown that two correlation lengths exist, one parallel to the direction of the path, and one perpendicular to it. These two correlation length are characterized by two exponents, ν_\perp and ν_\parallel . In two dimensions, $\nu_\perp = 1$. On the hierarchical lattice, only one such exponent can be defined, ν_\parallel , which we call ν from now on. To make the connection with the work of refs. 8 and 9, $\nu = 1/(\omega - 1)$.

In the above-mentioned case of the one-dimensional lattice, the small-disorder case corresponds to the central limit theorem. In this case, the distribution f_n approaches a Gaussian, i.e., $\varphi(x) \propto \exp[-x^2/(2\sigma^2)]$. In this case, the mean is invariant, so that $b = 0$, and the scale factor a appears in the scaling of the variance with the lattice size [Eq. (16)]: $a = \sqrt{2}$.

4.2. Iteration Transformations

In order to get some insight on the form of the relevant function φ for the minimal path problem, we use a steepest descent method. Let us write the initial distribution $f(x)$ in the form $f(x) = \exp[g(x)]$ and assume that the distribution g is concave, $d^2g(x)/dx^2 < 0$. It seems that this property is always valid asymptotically, and we assume that it is valid from the beginning. The \mathcal{S} transformation reads:

$$\phi(y) = \int_{-\infty}^{\infty} \exp[g(y-x) + g(x)] dx \quad (23)$$

Using the steepest descent method, we can estimate this integral as being controlled by the maximum of the argument of the exponential. This is achieved at the point x where $g'(x) = g'(y-x)$. Since g is assumed to be concave, the maximum is reached for $x = y/2$. Thus

$$\phi(y) = \exp[2g(y/2)] \quad (24)$$

The \mathcal{P} transformation [Eq. (12)] can now be performed. Two cases have to be distinguished. Let us call z_0 the point where ϕ reaches its maximum. If $z \ll z_0$, then the integral $\int_z^{\infty} \phi(y) dy$ can be considered as being constant and equal to 1. Thus,

$$\psi(z) = 2 \exp[2g(z/2)] \quad \text{for } z \ll z_0 \quad (25)$$

If $z \gg z_0$, then the integral $\int_z^{\infty} \phi(y) dy$ is dominated by its lower bound, and thus

$$\psi(z) = 2 \exp[4g(z/2)] \quad \text{for } z \gg z_0 \quad (26)$$

Finally the rescaling \mathcal{L} gives

$$\begin{aligned} \zeta(z) &= 4 \exp[2g(z)] & \text{for } z \ll z_0/2 \\ \zeta(z) &= 4 \exp[4g(z)] & \text{for } z \gg z_0/2 \end{aligned} \quad (27)$$

We can use now the asymptotic property of Eq. (19), which consists in

identifying the resulting ζ distribution with $\exp[g(ax + b) + \log(a)]$. We can identify the large- x behavior of the fixed point distributions $g(x)$.

Let us now investigate the stability of various form of behavior of g close to $+\infty$ or $-\infty$. The one-dimensional case suggests that we look at a power-law behavior first.

4.3. Power-Law Decay at $+\infty$

We will first show that the distribution of weight decays at $+\infty$ faster than any power law. Let us consider an initial distribution such that $f_0 \propto x^{-\mu-1}$ for $x \rightarrow \infty$. We cannot use directly Eq. (23) since $g(x)$ is not convex. However, it is easy to show that such a power-law tail is stable upon convolution (addition of two lattices in series or \mathcal{S} transformation). However, the \mathcal{P} transformation will change the exponent μ into

$$\mu' = 2\mu \tag{28}$$

Thus, after one generation, $f(x)$ behaves as $x^{-\mu'-1}$ at infinity. Upon iteration of the transformation, μ will tend to infinity. Therefore, a stable distribution will converge to zero at plus infinity faster than any power-law. This is to be contrasted with the one-dimensional case, where we have seen that the Lévy distributions—i.e., with power-law decay at infinity with exponents less than three—are stable.

Let us note that formally the case $\mu = 0$ is an unstable fixed point of the transformation equation (28). This limit is unphysical, since a probability distribution converges faster than x^{-1} at infinity. We will see in a following section that the limit $\mu \rightarrow 0^+$ has a simple physical interpretation as a percolation limit.

4.4. Power-Law Decay at $-\infty$

Let us now assume that $f(x) \propto (-x)^{-\mu-1}$ for $x \rightarrow -\infty$. In such a case, we see that the complete \mathcal{LPP} transformation preserves the power-law decay at infinity. In such a case, the sum of two variables will on average be controlled by the value of the smallest variable. Thus we can formally change the “min” operation into a sum. We now have a situation similar to the one-dimensional case. At each generation, we take the minimum (or the sum) of four elements and divide it by two. Thus, the scaling of the moments is trivial. The asymptotic distribution has a power-law tail at $-\infty$ and a rapid decay at $+\infty$. The second moment of the distribution will scale with the lattice size as

$$\sigma(L) \sim \sigma_0 L^{2/\mu-1} \tag{29}$$

The difference with Eq. (17) is that the number of elements considered is equal to L^2 , but we only rescale the result by a factor L . In order to find the largest value of $\mu = \mu_+$ which is stable, we will match the result (29) with that corresponding to a small-disorder case. Since we will argue below that $\nu = 3/2$, we obtain

$$2/\mu_+ - 1 = -1/\nu \quad (30)$$

or

$$\mu_+ = \frac{2\nu}{\nu - 1} = 6 \quad (31)$$

The first moment of the distribution will follow a behavior similar to the small-disorder case for less restrictive conditions than $\mu > \mu_+$. Indeed, the mean $\langle \alpha(L) \rangle$ will scale with L for low values of μ as $\langle \alpha \rangle \sim -L^{2/\mu - 1}$, in a regime where the value of α will be dominated by that of the smallest element in the network. A crossover to a small-disorder regime will take place for values of μ larger than μ_{++} such that $2/\mu_{++} - 1 = 0$ or $\mu_{++} = 2$.

Let us summarize this last result: Three types of regime are found, depending on the exponent μ .

(a) $\mu > \mu_+$. This case is not stable. The distribution will fall in the case of a small disorder, which we will analyze in more detail below.

(b) $\mu_{++} < \mu < \mu_+$. In this intermediate range, the first moment is proportional to the length of the path, but the fluctuations decay more slowly than in the small-disorder case.

(c) $\mu < \mu_{++}$. In this case, the norm of the path is no longer proportional to the length of the path, but scales with an exponent $2/\mu - 1$. The fluctuations are of the same order of magnitude as the mean.

To find a physical interpretation of these different regimes, it is more natural to change the weights into their opposite, so as to be able to deal only with positive numbers. Thus, the minimal path will be changed into a maximal path. The problem can still be mapped onto a directed polymer problem, but in a medium which attracts the polymer instead of being repulsive. In the second regime, the wandering of the polymer is larger than in the small-disorder case, *at all length scales*. The last regime is a case where the energy of the polymer is no longer proportional to the length of the polymer, but increases faster (as in the one-dimensional problem).

It is hard to find a corresponding Eden model or aggregation model which could be mapped onto a maximal path instead of a minimal path. However, if such a model could be constructed, then the second case,

$\mu_{++} < \mu < \mu_+$, would be such that the roughness of the interface is larger than in the small-disorder case, but it would still be confined to the external skin of the cluster, which would be dense. The last regime, $\mu < \mu_{++}$, would be such that the roughness of the cluster surface is scaling like the size of the cluster (like, e.g., for diffusion-limited aggregation, DLA). Thus, the boundary would contain fjords reaching the heart of the cluster. In this regime one might also expect that the cluster would then be fractal and no longer dense. Clearly such a behavior is reminiscent of the dielectric breakdown model introduced by Niemeyer *et al.*,⁽¹²⁾ where, by varying one parameter, it is possible to interpolate between the Eden model (which can be shown to be equivalent to the small-disorder case of the minimal path problem^(2,13)) and more ramified fractal clusters such as DLA clusters. It would be of great interest to see whether such a correspondance is only to be considered as illustrative or if it hides a deeper link.

4.5. Small Disorder

Let us now consider the small-disorder case where the initial distribution decays faster than $(-x)^{-\mu_+ - 1}$ [or $(-x)^{-7}$] at $-\infty$. Since in this case, the power laws on either plus or minus infinity are not stable, we look for asymptotic behaviors in the form of exponentials of power laws. For x much larger or much smaller than the maximum of f , we consider a power-law behavior for g , $g(x) \sim -|x|^{\gamma_{\pm}}$, with γ_+ and γ_- respectively for x large and small. This form satisfies the expected condition (19), provided

$$k_{\pm} |z|^{\gamma_{\pm}} = |az|^{\gamma_{\pm}} \tag{32}$$

where $k_+ = 2$ and $k_- = 4$, as can be read from Eq. (27). Equation (32) is simply the rewriting of Eq. (19) up to the dominant terms for large $|z|$. Therefore, we obtain

$$\begin{aligned} \gamma_+ &= \frac{\log(2)}{\log(a)} = \nu \\ \gamma_- &= \frac{\log(4)}{\log(a)} = 2\nu \end{aligned} \tag{33}$$

The conclusion of this subsection is that in the small-disorder regime, the behavior of the distribution $f(x)$ is $f(x) \propto \exp(-|x|^{\nu})$ for large x , and $f(x)$ is $f(x) \propto \exp(-|x|^{2\nu})$ for small x .

It is useful to compare this result with the similar one relative to the sum of random variables (one-dimensional problem). In the latter case, the fixed points of the convolution operator are given, in Fourier space, by

exponentials of power laws. In the minimal path problem, the major difference is that, in real space, the exponent is different according to the position with respect to the most probable value. Now, in order to conclude, we have to investigate the *stability* of these laws.

5. SMALL DISORDER

In order to find out the value of the exponent γ_{\pm} , we will establish a correspondence between the original problem in real space and its “Laplace” transform. We use here Laplace transform between quotes since we use the following transformation on a function $f(x)$:

$$\mathbf{L}f(s) = \int_{-\infty}^{+\infty} e^{-sx} f(x) dx \quad (34)$$

which is close to the usual Laplace transform, but in which the lower bound in the integral is $-\infty$ instead of 0. The usual Laplace transform cannot be used here since the functions we will deal with are nonzero from $-\infty$ to $+\infty$. However, most properties of the Laplace transform hold. For simplicity, we will refer to this transformation as a Laplace transform in the rest of the paper. The functions to which we will apply this transformation are supposed to be of the form established previously, i.e., with an exponential of power-law behavior at $\pm\infty$. This form ensures that the Laplace transform defined above will exist and be defined for all values of s .

The two main operations, \mathcal{L} and \mathcal{P} , can be simplified using appropriate transformations. Since the series transformation is a convolution product [see Eq. (10)] in Laplace space, the transform of the distribution is simply squared. The parallel transformation, Eq. (12), may be rewritten

$$\psi(z) = 2\varphi(z) \int_z^{\infty} \varphi(y) dy = \frac{d}{dz} \left(\int_z^{\infty} \varphi(y) dy \right)^2 = \mathbf{I}^{-1} \mathbf{2} \mathbf{I} \varphi(z) \quad (35)$$

where we have used the notation \mathbf{I} for the integral \int_z^{∞} and $\mathbf{2}$ for the square operation. In both cases, we apply a linear transformation—Laplace L or integral \mathbf{I} —then square the result, and apply the reverse transformation—inverse Laplace L^{-1} or derivative \mathbf{I}^{-1} . Omitting the rescaling (\mathcal{L}), one generation of transformation can be expressed as

$$\mathbf{I}^{-1} \mathbf{2} \mathbf{I} L^{-1} \mathbf{2} L \quad (36)$$

The exponents γ_{\pm} will not be changed through the transformation $\mathbf{I}^{-1} \mathbf{2} \mathbf{I}$. Therefore we simplify this transformation and turn it into a simple square

operation **2**. The resulting transformation now simply consists in square operations in real space and Laplace space, alternatively. We now note that the inverse Laplace transform can be identified with the Laplace transform itself, since we are only interested in a very crude characterization of the fixed point functions (namely the two exponents of the power law, which are the arguments of the exponential at plus or minus infinity). These two simplifications lead to the following transformation when going from one generation to the next:

$$\mathbf{2L2L} \tag{37}$$

Under the assumption that *the simplification of Eq. (36) into Eq. (37) does not affect the characteristic features of the fixed points*, we are able to compute the exponent ν . Indeed, we note that after the **2L** transformation, the resulting function will share the same properties as the fixed point itself, or $\mathbf{2L}\varphi(x) = \varphi(x)$, where the “=” sign should be taken here with a weak sense, i.e., that the two asymptotic behaviors of the functions close to $\pm\infty$ are the same.

To conclude, we need to know the behavior of $\mathbf{2L}\varphi(x)$ close to infinity, knowing that of $\varphi(x)$. Using again the steepest descent method, it is straightforward to get the following asymptotic behavior:

$$\mathbf{2L}\varphi(x) \sim \exp(-|s|^{\kappa_{\pm}}) \tag{38}$$

with κ_+ and κ_- , respectively, for s close to $+\infty$ and $-\infty$. These exponents are related to γ_{\pm} through

$$\kappa_{\pm} = \frac{\gamma_{\mp}}{\gamma_{\mp} - 1} \tag{39}$$

The identification $\mathbf{2L}\varphi(x) = \varphi(x)$ leads to $\kappa_{\pm} = \gamma_{\pm}$. Using the additional relation $\gamma_- = 2\gamma_+$ [Eq. (33)], we find

$$\gamma_+ = \frac{\gamma_+}{2(\gamma_+ - 1)} = \frac{3}{2} \tag{40}$$

and thus $\gamma_- = 3$.

This mapping allows us to determine the asymptotic behaviors of φ , as well as the scaling properties of the first and second moments of the minimal path problem, since we established that $\gamma_+ = \nu$ and thus $\nu = 3/2$. Let us underline that this result is only valid if our simplification does not change the nature of the fixed point.

Finally, this last proposal justifies the upper limit of $\mu_+ = 6$ leading to stable laws with a power-law tail at $-\infty$ as claimed previously [Eq. (31)].

It is remarkable to note that the value $\nu = 3/2$ that we suggest for the hierarchical lattice is identical to the result of two-dimensional *Euclidian* lattices.⁽⁴⁾ This result is surprising since generally the results obtained on hierarchical structures can only be qualitatively compared to those relative to Euclidian ones. We will see, for instance, that for the limit case of percolation, the correlation length exponents—which do exist in both cases—are nevertheless different ($\nu = 1.635$ and $\nu = 4/3$, respectively, for the hierarchical and the two-dimensional Euclidian lattices). It seems that the minimal path problem is less sensitive to the topology of the network than percolation.

6. THE LIMIT CASE OF PERCOLATION

We argued in the introduction that by varying the parameter a in the norm of paths, one could go continuously from a minimal path problem to a percolation one. However, it is possible to obtain the continuous change while keeping the same norm, say with $a = 1$ in Eq. (3). This is achieved by performing the following change of variable: $y = x^a$ in Eq. (3). The corresponding distribution of y , $h(y) dy$, is related to that of x through $h(y) = (1/a) f(y^{1/a}) y^{(1/a)-1}$. The percolation case is obtained in the limit $a \rightarrow +\infty$. As claimed previously, we see that in this case $h(y)$ approaches $1/y$, which is a ill-defined limit, since $1/y$ is not integrable to infinity. However, we may consider a finite a and let it go to infinite, or alternatively, consider a $1/y$ distribution for y in an interval, say $[1, A]$, and let A go to infinity. We are interested in the properties of infinite-size systems. In this particular case, care has to be taken with the ordering of the two limits $L \rightarrow \infty$ and $A \rightarrow \infty$. Taking first the limit of an infinite-size system will lead to the small-disorder case.

The easiest way to study this limit is, however, to use the norm that corresponds to percolation, i.e., $\|\dots\|_\infty$. We can perform an analysis similar—although simpler—to the one done previously in the minimal path problem. The series transformation now consists in taking the maximum of two numbers, $y = \max(x_1, x_2)$. The distribution of y is related to that of x by

$$\begin{aligned} \phi &= \mathcal{P}(f) \\ \phi(y) &= 2f(x) \int_{-\infty}^y f(x) dx \end{aligned} \tag{41}$$

The \mathcal{P} transformation remains identical to Eq. (12). The \mathcal{L} should no longer be considered, since no rescaling is needed. Working with the

integral distribution $F(x) = \int_{-\infty}^x f(x') dx'$ simplifies the computation, since the $\mathcal{P}\mathcal{S}$ transformation gives

$$\mathcal{P}\mathcal{S}F(x) = 1 - [1 - F(x)^2]^2 = [2 - F(x)^2] F(x)^2 \tag{42}$$

We find very simply the percolation threshold p_c of the hierarchical lattice using Eq. (7) and the transformation (42):

$$p_c = (2 - p_c^2) p_c^2 \tag{43}$$

or $p_c = (\sqrt{5} - 1)/2 \approx 0.618$. The shape of the asymptotic distribution $\varphi(x)$ can be obtained as previously by writing $\varphi(x) = \exp[g(x)]$ and using twice the result expressed in Eqs. (25) and (26). After one generation, the distribution $\zeta(x)$ is simply

$$\zeta(x) = 2 \exp[2g(x)] \tag{44}$$

For large arguments, the behavior of $g(x)$ is a power law: $g(x) \sim |x|^\gamma$. Equation (44) gives the relation between γ and the rescaling factor a of Eq. (19),

$$2 |x|^\gamma = |ax|^\gamma \tag{45}$$

or

$$\gamma = \frac{\log(2)}{\log(a)} = \nu \tag{46}$$

where the ν exponent is the percolation correlation length exponent (21) and (22), which is different from the previously discussed ν relative to the minimal path problem. The value of ν for percolation can be computed from the evolution of $F(x) = p$ for p close to but different from the percolation threshold p_c . In this case, after one generation, the rescaled p , written p' , is given by an equation similar to Eq. (43):

$$p' = 1 - (1 - p^2)^2 \tag{47}$$

For $p = p_c + \varepsilon$, and $\varepsilon \ll 1$, to first order in ε , we can write

$$p' - p_c = \left. \frac{\partial p'}{\partial p} \right|_{p_c} \varepsilon = \lambda \varepsilon \tag{48}$$

where $\lambda = 4p_c^2$ —we have used Eq. (43) to simplify the expression of λ . Using Eq. (20) with $b = p_c$, we identify $\alpha = \lambda$; thus,

$$\nu = \gamma = \frac{\log(2)}{\log(4p_c^2)} \tag{49}$$

Numerically, $\nu \approx 1.635$. Let us note that in this case, the value of the correlation length exponent ν is different from that of Euclidian lattice of the same dimension—two—where $\nu = 4/3$.⁽¹⁰⁾

7. NUMERICAL RESULTS

We have carried out numerical simulations of the minimal path problem searching for the invariant distribution under rescaling. We discretized the unknown function $\varphi(x)$ and iterated the transformations \mathcal{LPS} until the resulting function was invariant within numerical accuracy. Figure 2 shows a semilog plot of the function φ starting from a uniform distribution of local weight between zero and one. As expected, the computed φ function was independent of the initial distribution, provided it converges to zero faster than $-x^{-\mu_+}$.

Figure 3 shows that $\varphi(x)$ indeed behaves as $\exp(-|x|^{-\gamma_{\pm}})$ at $\pm\infty$. From the graph, we can measure the best slopes of linear regression of $\log\{-\log[\varphi(x)]\}$ versus $\log|x|$. We found $\gamma_- \approx 1.45$ and $\gamma_+ \approx 2.6$. Both estimates are a little smaller than the expected result $3/2$ and 3 . However, from the curvature of these plots, we can deduce that the measured exponents are certainly lower bounds of the asymptotic values, and thus they are consistent with our expectation within error bars. We also note that the curvature for γ_+ is much stronger than that for γ_- .

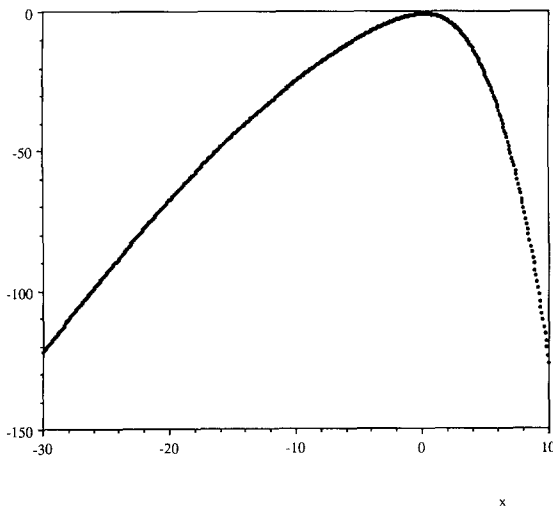


Fig. 2. Semilog plot of the asymptotically stable distribution, $\log[\varphi(x)]$, versus x for a small-disorder case. The mean has been fixed to zero and the second moment to one.

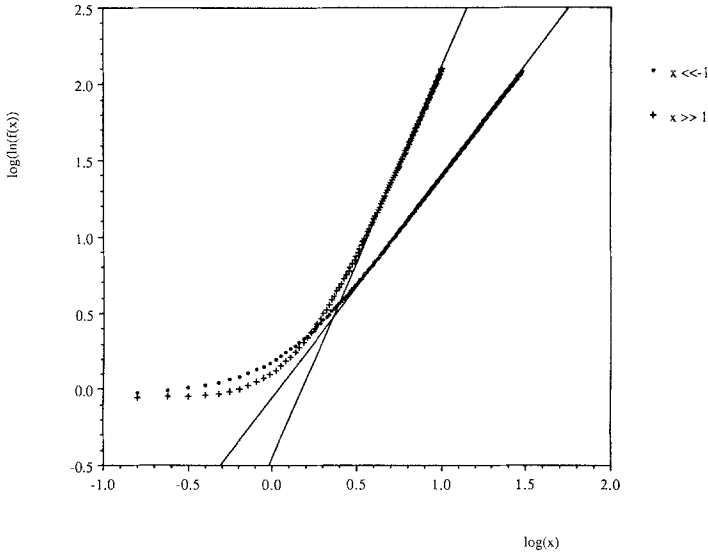


Fig. 3. Log-log plot of Fig. 2, $\log\{-\log[\phi(x)]\}$, versus $\log|x|$, relative to negative $x(\bullet)$ and positive $x(+)$. The lines drawn on the graph are best fits.

We also measured the second cumulant of the distribution and we found that it was rescaled from one generation to the next by a constant amount, $a \approx 1.62$, which leads to a direct estimate of $\nu = \log(2)/\log(a) \approx 1.43$. Once again, ν appears to be slightly underestimated. Direct Monte Carlo estimates of ν also lead to estimates of the order of 1.4. Such a value, $\nu = 1.425$, has also been obtained numerically by Derrida and Griffiths⁽⁸⁾ and Halpin-Healy.⁽⁹⁾ We have no argument to explain or to justify a systematic underestimate of ν numerically.

We tested the stability of power laws close to $-\infty$. In order to do so, we simply performed Monte Carlo simulations with a distribution $f_0(x) = \mu(-x)^{-1-\mu}$ for $x < -1$, with different values of μ . Let us mention a technical detail: The distribution of this mean value is such that the measured mean is expected to depend on the number of samples on which the data have been generated. In order to avoid this spurious statistical effect, we estimated the arithmetic mean on ten realizations of a given system size, and then we took the *harmonic* mean over different sets of ten realizations. The same holds for our estimates of the variance σ . The number of realizations in the same set is kept constant (equal to ten) for all system sizes. However, the number of these sets decreases as the system size increases. We considered one set a generation ten, four sets at generation nine, sixteen sets at generation eight, etc.

Figure 4 shows the log-log plot of the mean value of $\alpha(L)$ as a function of the lattice size for $\mu = 1, 2$, and 4. The prediction of Section 4 is that for μ less than 2, $\alpha(L)$ will scale as the lattice size to the power $2/\mu - 1$, whereas for μ larger than 2, $\alpha(L)$ should stay constant. For $\mu = 1$, we obtain a power law with an exponent measured to be 1.03, consistent with the expectation 1. For $\mu = \mu_{++} = 2$, the curve displays a clear downward curvature, indicating an exponent smaller than the tangent slope of the graph at the larger L considered, i.e., smaller than 0.14. This is again consistent with the expected result 0. For $\mu = 4$ the graph indicates a tangent exponent of the order of 0.03 for large system sizes, again in agreement with 0.

We report the estimates of the deviation $\sigma(L)$ as a function of the lattice size in Fig. 5, for $\mu = 1, 2$, and 4. We expect a power-law behavior with an exponent $2/\mu - 1$, or, respectively, 1, 0, and -0.5 . Omitting the largest system size because of statistical uncertainty, and the two smaller to avoid size effects, we measure, respectively, 1.04, 0.03, and -0.49 . The agreement is quite satisfactory.

Finally, we have studied numerically the case of percolation as explained above so as to obtain the invariant distribution $\varphi(x)$. We show in Fig. 6 the resulting function plotted as in Fig. 3. We expect to obtain for large arguments x (either positive or negative) a power-law behavior with an exponent $\nu \approx 1.635$ [Eq. (49)]. We see a slightly different behavior for

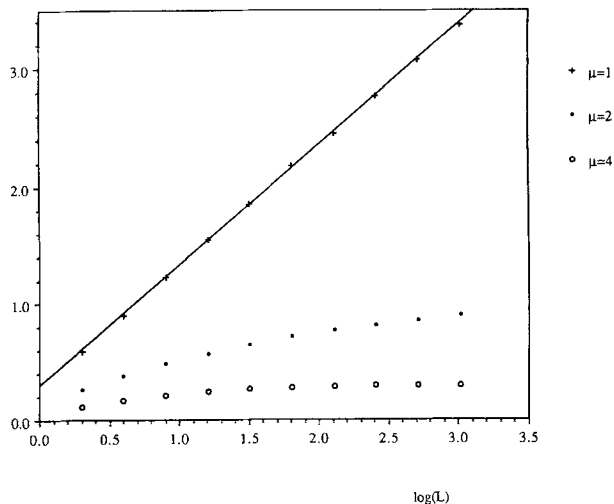


Fig. 4. Log-log plot of the mean value of $\alpha(L)$ as a function of the lattice size L with distributions of local weights such that $f_0(x) = \mu(-x)^{-\mu-1}$ for $x < -1$. Three values of μ are shown on the graph: $\mu = 1(+)$; $\mu = 2(\bullet)$; and $\mu = 4(\circ)$.

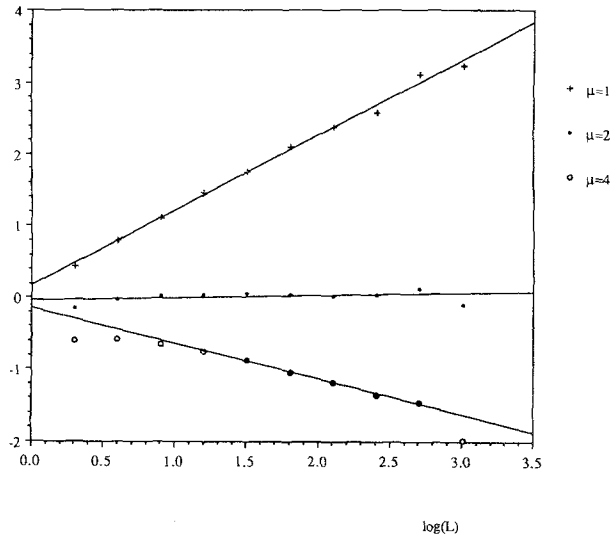


Fig. 5. Log-log plot of the deviation of $\alpha(L)$, $\sigma(L)$, as a function of the lattice size L with distributions of local weights such that $f_0(x) = \mu(-x)^{-\mu-1}$ for $x < -1$. Three values of μ are shown on the graph: $\mu = 1(+)$; $\mu = 2(\bullet)$; and $\mu = 4(\circ)$. The straight lines are best fits.

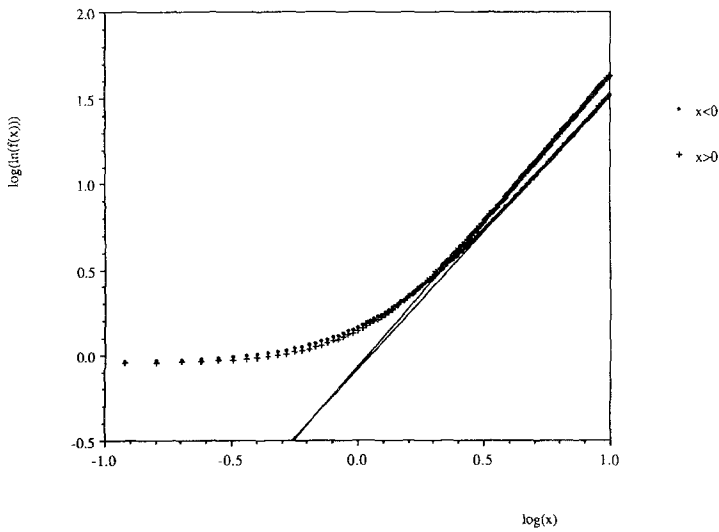


Fig. 6. Same as Fig. 3, for the percolation case. Results are for positive values of x (+) and negative ones (•). The two curves are expected to approach a straight line of slope γ in both cases. The lines drawn on the graph are best fits.

positive and negative values. The measured slopes are equal to 1.71 and 1.61 for positive and negative x , respectively. The estimate of the rescaling parameter a from one generation to the next is given by a direct integration of the function provided the estimate $\nu = 1.644$. The differences between the theoretical predictions and the numerical estimates lie within the error bars.

8. BREAKDOWN OF UNIVERSALITY FOR MAXIMAL PATHS

After most of this work was completed, we became aware of a recent numerical study by Zhang,⁽¹⁴⁾ who investigated the role of a power-law tail in the distributions of local weights (for positive values) for *maximal* directed paths in a two-dimensional medium. This is simply equivalent to studying power-law tails for negative weights for *minimal* paths as we have done previously (Section 4.4). Zhang reported that the values of the critical exponents governing the scaling properties of the path were very sensitive to the value of the power-law exponent μ . In this reference, two exponents were studied, χ and z , which can be related to our ν through

$$\begin{aligned}\chi &= \frac{2(\nu - 1)}{2\nu - 1} \\ z &= \frac{2\nu}{2\nu - 1}\end{aligned}\tag{50}$$

The range of values investigated in this reference was $2 \leq \mu \leq 7$. The exponent χ was found to tend toward 1 as μ approached 2, and to decrease for larger μ .

This trend is similar to our finding for the hierarchical lattice, where

$$\chi = \frac{4}{\mu + 2}\tag{51}$$

for $2 = \mu_+ \leq \mu \leq \mu_{++} = 6$ and $\chi = 1/2$ for $\mu \geq 6$. A quantitative agreement with the numerical results of ref. 12 is found for μ smaller than 4, but rather large deviations are found for μ larger than 5. In particular, the usual set of exponents is not recovered for $\mu = 6$, nor even $\mu = 7$.

This result by Zhang, termed “nonuniversality,” has received a considerable attention, and several studies by different groups deal with this problem. In particular, a very accurate numerical analysis of this problem was performed by Amar and Family⁽¹⁵⁾ in a two-dimensional Euclidian lattice. Their numerical estimates of the two exponents χ (called α in this

reference) and z are in very close agreement with our finding on the hierarchical lattice.

Zhang⁽¹⁶⁾ and Krug⁽¹⁷⁾ independently proposed a Flory approach to the problem which gives a different prediction, $\chi = 3/(\mu + 1)$, and thus $\mu_+ = 5$. This relation seems to be ruled out by the numerical results of Amar and Family.⁽¹⁵⁾

It is also important to note that the different stable behaviors observed for the minimal path problem have no consequence on the universality of the Eden model, since it can be shown⁽¹³⁾ that this model can be mapped exactly onto the minimal path one, with only *positive* weights. Moreover, the distribution of these weights, which can be computed exactly, is an exponential distribution, thus with no power-law tail at infinity.

9. CONCLUSION

We have presented a complete scaling picture of the minimal path problem on the hierarchical lattice for all distributions of random weights: we have identified the different limit behaviors [power-law tail at minus infinity (Section 4.4) and small-disorder case (Section 4.5)], their basin of attraction (dictated by the power-law behavior close to minus infinity of the initial distribution), and the asymptotic shape of the distribution of minimal weight for the small-disorder case, and for the extreme-disorder case (percolation). We have also presented an argument—which relies on the assumption that a simplification of the renormalization does not affect the large-argument behavior of the distribution—which gives the result $\nu = 3/2$ for the hierarchical lattice. The results of numerical simulations support the presented analysis, although the value of ν seems to be systematically smaller than the predicted value of $3/2$.

In the light of the striking agreement that we observe between the exact results on the hierarchical lattice and the observed numerical results on Euclidian lattices concerning the stability of power-law tails close to minus infinity, it seems that the simple topology of the first case does not affect the overall behavior. Deeper understanding of this puzzling observation would be desirable.

ACKNOWLEDGMENTS

S.R. acknowledges the hospitality of the University of Rio Grande do Norte, where most of this work was performed. We thank A. Aharony, J. Feder, E. Guyon, H. J. Herrmann, E. L. Hinrichsen, and T. Jøssang for fruitful discussions. This work was motivated by a question raised by B. Derrida in *Stat. Phys.* 17.⁽¹⁸⁾

REFERENCES

1. M. Kardar, G. Parisi, and Y. C. Zhang, *Phys. Rev. Lett.* **56**:889 (1986).
2. M. Kardar and Y. C. Zhang, *Phys. Rev. Lett.* **58**:2087 (1987).
3. S. Roux, A. Hansen, and E. Guyon, *J. Phys. (Paris)* **48**:2125 (1987).
4. D. A. Huse and C. L. Henley, *Phys. Rev. Lett.* **54**:2708 (1985); M. Kardar, *Phys. Rev. Lett.* **55**:2923 (1985); D. A. Huse, C. L. Henley, and D. S. Fisher, *Phys. Rev. Lett.* **55**:2924 (1985).
5. D. E. Wolf and J. Kertész, *Europhys. Lett.* **4**:651 (1987).
6. A. J. McKane and M. A. Moore, *Phys. Rev. Lett.* **60**:527 (1988).
7. J. M. Kim and J. M. Kosterlitz, *Phys. Rev. Lett.* **62**:2289 (1989); D. E. Wolf and J. Kertész, *Phys. Rev. Lett.* **63**:1191 (1989); J. M. Kim and J. M. Kosterlitz, *Phys. Rev. Lett.* **63**:1192 (1989).
8. B. Derrida and R. B. Griffiths, *Europhys. Lett.* **8**:111 (1989).
9. T. Halpin-Healy, *Phys. Rev. A* **42**:711 (1990); *Phys. Rev. Lett.* **63**:917 (1989).
10. D. Stauffer, *Introduction to Percolation Theory* (Taylor and Francis, London, 1987).
11. J. P. Bouchaud and A. Georges, *Phys. Rep.*, to appear.
12. L. Niemeyer, L. Pietronero, and H. J. Weismann, *Phys. Rev. Lett.* **52**:286 (1984).
13. S. Roux, A. Hansen, and E. L. Hinrichsen, *J. Phys. A* **24**:L295 (1991).
14. Y. C. Zhang, *J. Phys. (Paris)* **51**:2129 (1990).
15. J. G. Amar and F. Family, *J. Phys. A* **24**:L79 (1991).
16. Y. C. Zhang, Preprint.
17. J. Krug, Preprint.
18. B. Derrida, *Physica A* **163**:71 (1990).